

Sound velocities and elastic properties of PbTiO_3 and PbZrO_3 under pressure: First principles study

Narasak Pandech^{a,b}, Kanoknan Sarasamak^c, Sukit Limpijumnong^{a,b,*}

^a*School of Physics, Suranaree University of Technology, Nakhon Ratchasima 30000, Thailand*

^b*Thailand Center of Excellence in Physics (ThEP Center), Commission on Higher Education, Bangkok 10400, Thailand*

^c*College of Nanotechnology, King Mongkut's Institute of Technology Ladkrabang, Bangkok 10520, Thailand*

Available online 16 October 2012

Abstract

The elastic constants and sound velocities as a function of pressure for perovskite materials PbTiO_3 (PTO) and PbZrO_3 (PZO) were investigated by first principles calculations. Under ambient pressure, the calculated structural parameters were calculated and found to be in good agreement with known values. To study properties under pressure, PTO and PZO were calculated at several reduced volumes, each of which corresponds to the system under pressure. The C_{11} , C_{12} and C_{44} elastic constants are all found to increase with pressure for the pressure range studied. Because the sound velocities are directly derived from the elastic constants, the relationships between the sound velocities and pressure also follow similar trends. The longitudinal modes are all larger than those of the transverse modes.

© 2012 Elsevier Ltd and Techna Group S.r.l. All rights reserved.

Keywords: D. Perovskite; First principles; Sound velocities

1. Introduction

PbZrO_3 (PZO) and PbTiO_3 (PTO) are the parent compound materials of the extensively utilized ferroelectric material $\text{Pb}(\text{Ti,Zr})\text{O}_3$ (PZT). PZT (as well as PZO and PTO) has perovskite structure and is used in many devices such as ultrasonic transducers and piezoelectric actuators [1]. The room temperature phase of PZO and PTO is orthorhombic and tetragonal structure, respectively [2,3]. Both orthorhombic PZO and tetragonal PTO have only slight distortion from the perfect cubic perovskite structure. Their elastic properties have been studied by several research groups. Liu et al. [4] theoretically studied the elastic properties of PTO in both cubic and tetragonal phases. Kalinichev et al. [3] used Brillouin light scattering to obtain the elastic and piezoelectric constants for tetragonal PTO single crystals at room temperature. For PZO,

Kagimura and Singh [2] studied the elastic properties and energetics of orthorhombic and rhombohedral phases.

Some effects of hydrostatic pressures on perovskite materials beside PTO and PZO have been experimentally and theoretically investigated. To our knowledge, the elastic properties and sound velocities of PTO and PZO under pressure have not been reported. For PTO, most of previous works were performed in order to understand their ferroelectric properties under ambient pressure. Liu et al. [4] focused mainly on the calculations of equilibrium tetragonal to cubic phase transition pressure of PTO. In this work, the elastic constants and sound velocities under pressure in cubic perovskite PZO and PTO were studied by using the density functional theory calculations.

2. Elastic properties of the cubic perovskite crystal

2.1. Elastic constants of the cubic perovskite crystal

Elastic constants of materials can be obtained by *ab-initio* calculations using two main approaches [5]. The first approach is based on the analysis of the total energies of the strained state of the materials which is

*Corresponding author at: School of Physics, Suranaree University of Technology, Nakhon

Ratchasima 30000, Thailand. Tel.: +66 4422 3000.

E-mail address: sukit@sut.ac.th (S. Limpijumnong).

called “energy–strain approach” [6]. Another approach is based on the analysis of the changes in calculated stress values resulting from the changes in the strain. This approach is called “stress–strain approach” [7].

In this work, the elastic constants (C_{ij}) were calculated by using the stress–strain approach. The stress–strain relation can be written in the matrix form as

$$\begin{pmatrix} \sigma_{xx} \\ \sigma_{yy} \\ \sigma_{zz} \\ \sigma_{yz} \\ \sigma_{zx} \\ \sigma_{xy} \end{pmatrix} = \begin{pmatrix} C_{11} & C_{12} & C_{13} & C_{14} & C_{15} & C_{16} \\ C_{21} & C_{22} & C_{23} & C_{24} & C_{25} & C_{26} \\ C_{31} & C_{32} & C_{33} & C_{34} & C_{35} & C_{36} \\ C_{41} & C_{42} & C_{43} & C_{44} & C_{45} & C_{46} \\ C_{51} & C_{52} & C_{53} & C_{54} & C_{55} & C_{56} \\ C_{61} & C_{62} & C_{63} & C_{64} & C_{65} & C_{66} \end{pmatrix} \begin{pmatrix} e_{xx} \\ e_{yy} \\ e_{zz} \\ e_{yz} \\ e_{zx} \\ e_{xy} \end{pmatrix} \quad (1)$$

where σ_{ij} ($i, j=x, y, z$) are the stress components, e_{ij} ($i, j=x, y, z$) are the strain components, and $C_{\lambda\alpha}$ ($\lambda, \alpha=1, 2, 3, \dots, 6$) are the elastic constants. For cubic perovskite structure, the 36 elastic constants in Eq. (1) can be reduced to three independent elastic constants because of the high symmetry of the structure. The three independent elastic constants are denoted by C_{11} , C_{12} and C_{44} . Eq. (1) is reduced to

$$\begin{pmatrix} \sigma_{xx} \\ \sigma_{yy} \\ \sigma_{zz} \\ \sigma_{yz} \\ \sigma_{zx} \\ \sigma_{xy} \end{pmatrix} = \begin{pmatrix} C_{11} & C_{12} & C_{12} & 0 & 0 & 0 \\ C_{12} & C_{11} & C_{12} & 0 & 0 & 0 \\ C_{12} & C_{12} & C_{11} & 0 & 0 & 0 \\ 0 & 0 & 0 & C_{44} & 0 & 0 \\ 0 & 0 & 0 & 0 & C_{44} & 0 \\ 0 & 0 & 0 & 0 & 0 & C_{44} \end{pmatrix} \begin{pmatrix} e_{xx} \\ e_{yy} \\ e_{zz} \\ e_{yz} \\ e_{zx} \\ e_{xy} \end{pmatrix} \quad (2)$$

2.2. Sound velocities of the cubic perovskite crystal

Sound velocities in materials are related to their elastic constants by a simple relationship:

$$v_P(\hat{q}) = \sqrt{C_P(\hat{q})/\rho} \quad (3)$$

where P indicates the polarization, which can be either L for longitudinal or T for transverse, and \hat{q} is the propagation direction of the wave. ρ is the mass density and $C_k(\hat{q})$

is the combination of elastic constants. The expression on the right hand side of Eq. (3) for three propagation directions of the cubic perovskite structure are summarized in Table 1.

3. Computational method

The computational approach employed was based on first principles density functional theory [8,9] with the plane wave pseudo-potential as implemented in Vienna *Ab-initio* Simulation Package (VASP) code [10]. For the exchange correlation terms, both local density approximation (LDA) [11,12] and generalized gradient approximation (GGA) [13] were used. The ultrasoft version of the pseudo-potential implemented in the VASP code allows a low cut off energies for the plane wave expansion of only 500 eV. We used a $8 \times 8 \times 8$ Monkhorst–Pack scheme [14] k -point sampling.

A cubic perovskite structure has the space group $Pm\bar{3}m(\#221)$ with the Wychoff positions: Pb 1a (0,0,0), Ti (or Zr) 1b (0.5,0.5,0.5) and O 3c (0,0.5,0.5), (0.5,0.5,0) and (0.5,0.0.5) as illustrated in Fig. 1.

The total energies (E) of a unit cell of the crystal at several slightly different volumes (V) were calculated and fitted into the equation of states [15] to obtain the bulk modulus (B_0) and its pressure derivative (B') of the crystal. In order to study the crystal properties under pressures, the elastic constants and sound velocities were calculated at several reduced volumes, following the approach described in Ref. [16]. The reduced crystal volume can be translated into the corresponding pressure following pressure–volume (P – V) relationship in the Birch–Murnaghan’s equation of state [17] written as

$$P(V) = \frac{3B_0}{2} \left[\left(\frac{V_0}{V} \right)^{7/3} - \left(\frac{V_0}{V} \right)^{5/3} \right] \left\{ 1 + \frac{3}{4}(B'-4) \left[\left(\frac{V_0}{V} \right)^{2/3} - 1 \right] \right\} \quad (4)$$

where V_0 is the equilibrium volume.

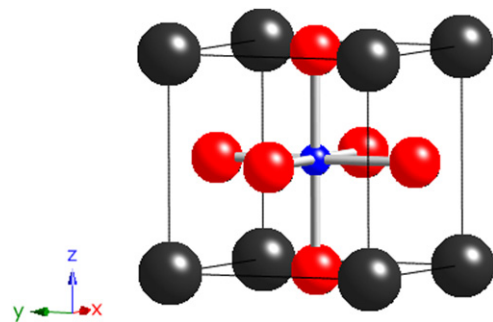


Fig. 1. Schematic illustration of a cubic perovskite unit cell. The dark gray spheres represent Pb atoms, blue sphere: Ti or Zr atom and red spheres: O atoms. (For interpretation of the references to color in this figure legend, the reader is referred to the web version of this article.)

Table 1
Sound velocity expressions of each wave propagation direction for the cubic structure.

Sound velocity	Expression
$v_L([100])$	$(C_{11}/\rho)^{1/2}$
$v_T([100])$	$(C_{44}/\rho)^{1/2}$
$v_L([110])$	$[(C_{11} + C_{12} + 2C_{44})/2\rho]^{1/2}$
$v_T([110])$	$[(C_{11} - C_{12})/\rho]^{1/2}$
$v_L([111])$	$[(C_{11} + 2C_{12} + 4C_{44})/3\rho]^{1/2}$
$v_T([111])$	$[(C_{11} - C_{12} + C_{44})/3\rho]^{1/2}$

4. Results and discussions

4.1. Structural and elastic properties at zero pressure

The calculated equilibrium lattice constants as well as the corresponding volumes of both PTO and PZO based on both LDA and GGA exchange correlation functional are compared to other computation and experimental results in Table 2. Our values are consistent with other calculated results. In comparison with the experimental values, LDA tends to give slightly too small lattice constants while GGA tends to give slightly too large values. This is consistent with what have been observed in other materials.

The bulk modulus (B), its pressure derivative (B') and the elastic constants at zero pressure of both PTO and PZO are also shown in Table 2. Because LDA gives smaller lattice constants compared to GGA, the bulk moduli and all elastic constants computed using LDA are consistently higher than those corresponding ones computed using GGA. PTO has been previously studied by Piskunov et al. [18] and Liu et al. [4]. Liu et al. values calculated based on LDA are very similar to ours. However, Piskunov et al. LDA results are consistently higher

than ours while their GGA results are quite similar. To our knowledge, there is no computation result available for PZO. The sound velocities, shown in the bottom section of Table 2, can be derived from the elastic constants using the expressions shown in Table 1.

4.2. Elastic properties under pressure

To study the elastic constants and sound velocities under hydrostatic pressures, the calculations were performed at several reduced volumes, each of which corresponds to the system under a different pressure. The pressure can be determined from the pressure–volume relation shown by Eq. (1). Sound velocities of PTO and PZO under pressure can be obtained from the corresponding elastic constants using the expressions given in Table 1.

The elastic constants as a function of pressure for cubic perovskite PTO and PZO are shown in Fig. 2. Both materials have similar behavior in the changes of elastic constants under pressure. In general, we can see that all three elastic constants, C_{11} , C_{12} and C_{44} increase with pressure. In both PTO and PZO, C_{11} , which is related to the longitudinal distortion, rapidly increases with pressure. On the other hand, C_{12} and C_{44} are much less sensitive to

Table 2

Calculated lattice constants (a) in Å, volumes (V_0) in Å³, bulk modulus (B) in GPa, its pressure derivative (B'), elastic constants in GPa and sound velocities in km/s of PbTiO₃ and PbZrO₃ in the cubic perovskite structure compared with literatures.

		PbTiO ₃		PbZrO ₃	
		LDA	GGA	LDA	GGA
a	Present	3.89	3.97	4.13	4.20
	Other calc.	3.88 ^a , 3.93 ^b	3.98 ^a , 3.96 ^b	4.11 ^c	4.19 ^c , 4.18 ^d
	Expt.	3.95 ^e		4.16 ^f	
V_0	Present	58.76	63.32	70.22	74.08
B	Present	219	185	181	168
	Other calc.	229 ^g , 324 ^b	213 ^b	–	–
B'	Present	4.5	3.5	4.6	3.7
C_{11}	Present	380	316	366	322
	Other calc.	384 ^g , 450 ^b	325 ^b	–	–
C_{12}	Present	145	130	92	89
	Other calc.	151 ^g , 261 ^b	158 ^b	–	–
C_{44}	Present	103	96	63	62
	Other calc.	120 ^g , 113 ^b	107 ^b	–	–
$v_L[100]$	Present	6.66	6.25	6.69	6.42
$v_T[100]$	Present	3.46	3.44	2.78	2.82
$v_L[110]$	Present	6.53	6.28	5.98	5.86
$v_T[110]$	Present	3.70	3.39	4.10	3.86
$v_L[111]$	Present	6.48	6.43	5.72	5.65
$v_T[111]$	Present	3.63	3.55	3.71	3.55

^aCalculations by Hosseini et al. [19].

^bCalculations by Piskunov et al. [18].

^cCalculations by Wang et al. [20].

^dCalculations by Baedi et al. [21].

^eMeasurements by Kuroiwa et al. [22].

^fMeasurements by Fujiishita et al. [23].

^gCalculations by Liu et al. [4].

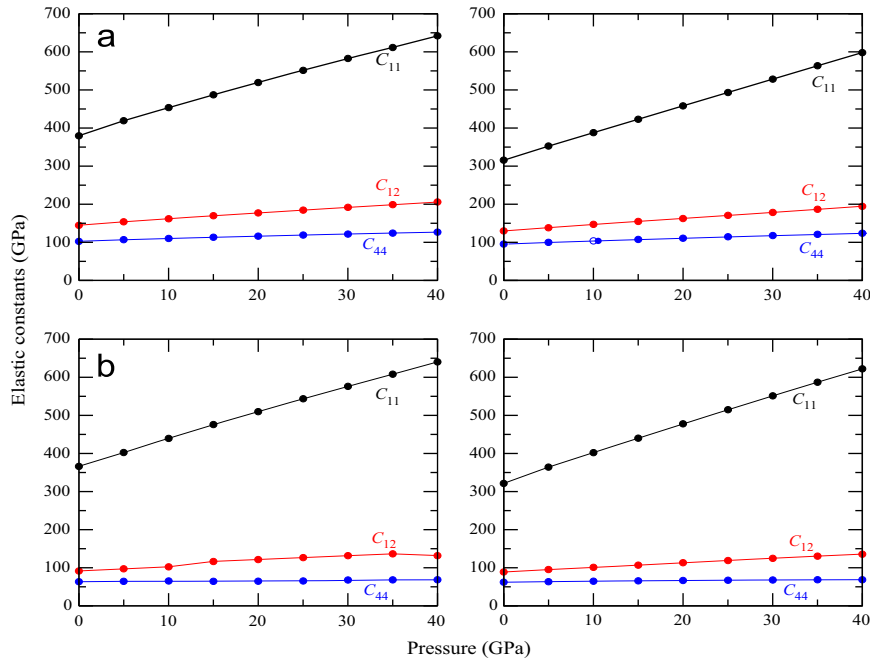


Fig. 2. Elastic constants as a function of pressure for cubic perovskite PbTiO_3 and PbZrO_3 , obtained from LDA (left) and GGA (right). (a) PbTiO_3 and (b) PbZrO_3 .

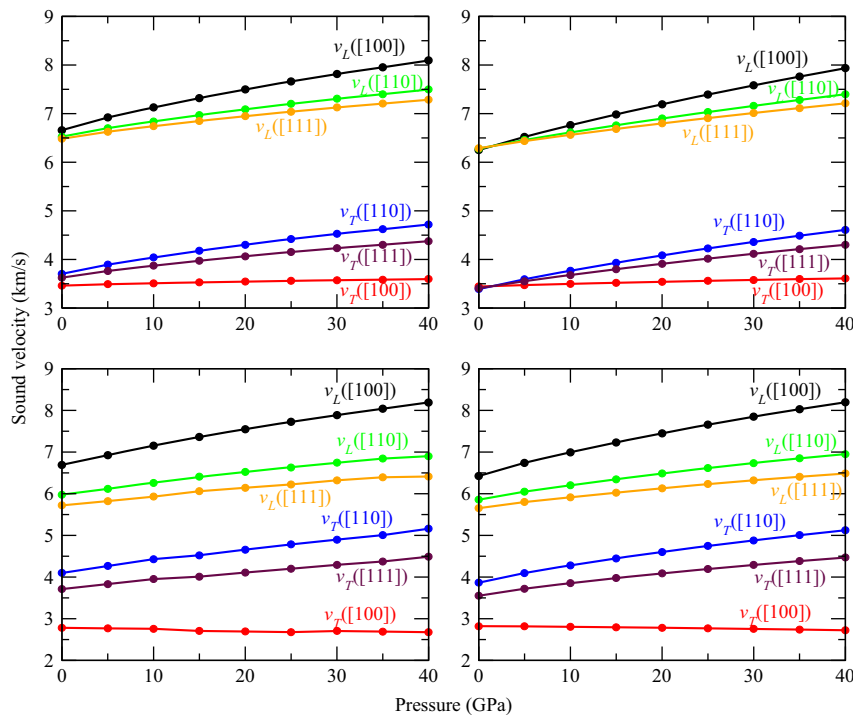


Fig. 3. Sound velocities as a function of pressure for cubic perovskite PbTiO_3 and PbZrO_3 , obtained from LDA (left) and GGA (right). (a) PbTiO_3 and (b) PbZrO_3 .

pressure. Indeed, C_{44} , which is related to the transverse distortion, remains almost flat. The calculated sound velocities under pressure for both cubic perovskite PTO and PZO are shown in Fig. 3. Since the sound velocities are directly derived from the elastic constants, a similar

trend was found. All of the sound velocities, except for the $v_T([100])$ of PZO, increase with pressure mainly because they contain C_{11} which rapidly increases with pressure. In PZO, $v_T([100])$ slightly decreases under pressure because it is associated only with C_{44} which remains almost flat

with pressure and divided by ρ which increases with pressure. As expected, the longitudinal modes are larger than the transverse modes such that they can be divided into two groups.

5. Conclusions

The elastic constants and sound velocities of perovskite PTO and PZO as a function of pressure were calculated by first principles calculations. Both LDA and GGA exchange and correlations were used. The calculated zero-pressure properties are in good agreement with the previous studies ensuring the validity of the results. LDA gives slightly smaller lattice constants and larger bulk moduli than GGA which is consistent with what have been observed in other materials. The elastic constants and sound velocities under the pressure range of 0–40 GPa were presented. The elastic constants are almost linearly increased with pressure. C_{11} rapidly increases with pressure while C_{12} and C_{44} are much less sensitive to pressure. Because the sound velocities are related to the elastic constants, almost all of them increase with pressure.

Acknowledgments

This work was partially supported by Development and Promotion of Science and Technology Talents Project (DPST, Thailand) and Thailand Center of Excellence in Physics (ThEP Center). Computations were carried out at the Synchrotron Light Research Institute, Thailand.

References

- [1] T. Yamamoto, Y. Makino, Pressure dependence of ferroelectric properties in PbZrO_3 – PbTiO_3 solid state system under hydrostatic stress, *Japanese Journal of Applied Physics* 35 (1996) 3214–3217.
- [2] R. Kagimura, D.J. Singh, First-principles investigations of elastic properties and energetics of antiferroelectric and ferroelectric phases of PbZrO_3 , *Physical Review B* 77 (2008) 104113.
- [3] A.G. Kalinichev, J.D. Bass, B.N. Sun, D.A. Payne, Elastic properties of tetragonal PbTiO_3 single crystals by brillouin scattering, *Journal of Materials Research* 12 (1997) 2623–2627.
- [4] Y. Liu, G. Xu, C. Song, Z. Ren, G. Han, Y. Zheng, First-principles study of elastic properties in perovskite PbTiO_3 , *Materials Science and Engineering A: Structural Materials, Properties, Microstructure and Processing* 472 (2008) 269–272.
- [5] Y. Le Page, P. Saxe, Symmetry-general least-squares extraction of elastic data for strained materials from ab initio calculations of stress, *Physical Review B* 65 (2002) 104104.
- [6] Y. Le Page, P. Saxe, Symmetry-general least-squares extraction of elastic coefficients from ab initio total energy calculations, *Physical Review B* 63 (2001) 174103.
- [7] O.H. Nielsen, R.M. Martin, First-principles calculation of stress, *Physical Review Letters* 50 (1983) 697–700.
- [8] P. Hohenberg, W. Kohn, Inhomogeneous electron gas, *Physical Review* 136 (1964) B864–B871.
- [9] W. Kohn, L.J. Sham, Self-consistent equations including exchange and correlation effects, *Physical Review* 140 (1965) A1133–A1138.
- [10] G. Kresse, J. Furthmüller, Efficient iterative schemes for ab initio total-energy calculations using a plane-wave basis set, *Physical Review B* 54 (1996) 11169–11186.
- [11] D.M. Ceperley, B.J. Alder, Ground state of the electron gas by a stochastic method, *Physical Review Letters* 45 (1980) 566–569.
- [12] J.P. Perdew, A. Zunger, Self-interaction correction to density-functional approximations for many-electron systems, *Physical Review B* 23 (1981) 5048–5079.
- [13] J.P. Perdew, K. Burke, M. Ernzerhof, Generalized gradient approximation made simple, *Physical Review Letters* 77 (1996) 3865–3868.
- [14] H.J. Monkhorst, J.D. Pack, Special points for brillouin-zone integrations, *Physical Review B* 13 (1976) 5188–5192.
- [15] J.H. Li, S.H. Liang, H.B. Guo, B.X. Liu, Four-parameter equation of state of solids, *Applied Physics Letters* 19 (2005) 194111–194113.
- [16] K. Sarasamak, S. Limpijumnong, W.R.L. Lambrecht, Pressure-dependent elastic constants and sound velocities of wurtzite SiC , GaN , InN , ZnO , and CdSe , and their relation to the high-pressure phase transition: a first-principles study, *Physical Review B* 82 (2010) 035201.
- [17] J.P. Poirier, *Introduction to the Physics of the Earth Interior*, second ed., Cambridge University Press, Cambridge, 2000.
- [18] S. Piskunov, E. Heifets, R.I. Eglitis, G. Borstel, Bulk properties and electronic structure of SrTiO_3 , BaTiO_3 , PbTiO_3 perovskites: an ab initio HF/DFT study, *Computational Materials Science* 29 (2004) 165–178.
- [19] S.M. Hosseini, T. Movlaroooy, A. Kompany, First-principle calculations of the cohesive energy and the electronic properties of PbTiO_3 , *Physica B* 391 (2007) 316–321.
- [20] Y.X. Wang, M. Arai, T. Sasaki, C.L. Wang, W.L. Zhong, First-principles study on the (001) surface of cubic PbZrO_3 and PbTiO_3 , *Surface Science* 585 (2005) 75–84.
- [21] J. Baedi, S.M. Hosseini, A. Kompany, E.A. Kakhki, Structural, electronics and optical properties of lead zirconate, *Physica Status Solidi B* 245 (2008) 2572–2580.
- [22] Y. Kuroiwa, S. Aoyagi, A. Sawada, J. Harada, E. Nishibori, M. Takata, M. Sakata, Evidence for Pb–O covalency in tetragonal PbTiO_3 , *Physical Review Letters* 87 (2001) 217601–217604.
- [23] H. Fujishita, Y. Ishikawa, S. Tanaka, A. Ogawaguchi, S. Katano, Crystal structure and order parameters in the phase transition of antiferroelectric PbZrO_3 , *Journal of the Physical Society of Japan* 72 (2002) 1426–1435.